Dynamics and Distant Effects of Frontal/Temporal Epileptogenic Focus using Functional Connectivity Maps

Hoda Rajaei, Mercedes Cabrerizo[*], Panuwat Janwattanapong, Alberto Pinzon, Sergio Gonzales-Arias, Armando Barreto, Jean Andrian, Naphtali Rishe, Ilker Yaylali and Malek Adjouadi

Abstract— Objective: **Connectivity patterns of interictal epileptiform discharges (IED) are all subtle indicators of where the 3D source of a seizure could be located. These specific patterns are explored in the recorded electroencephalogram (EEG) signals of 20 individuals diagnosed with focal epilepsy to assess how their functional brain maps could be affected by the 3D onset of a seizure.** *Methods:* **Functional connectivity maps, estimated by phase synchrony among EEG electrodes, were obtained by applying a data-driven recurrence-based method. This is augmented through a novel approach for selecting optimal parameters that produce connectivity matrices that are deemed significant for assessing epileptiform activity in context to the 3D source localization of seizure onset. These functional connectivity matrices were evaluated in different brain areas to gauge the regional effects of the 3D epileptic source.** *Results:* **Empirical evaluations indicate high synchronization in the temporal and frontal areas of the effected epileptic hemisphere, while strong links connect the irritated area to frontal and temporal lobes of the opposite hemisphere.** *Conclusion:* **Epileptic activity originating in the temporal or frontal areas is seen to affect these areas in both hemispheres.** *Significance:* **The results obtained express the dynamics of focal epilepsy in context to both the epileptogenic zone and the affected distant areas of the brain.**

Index Terms— **Electroencephalography (EEG), Epileptogenic zone, Focal epilepsy, Functional connectivity, Interictal epileptiform discharges (IED), Nonlinear recurrence-based methods.**

I. INTRODUCTION

Epilepsy is a chronic neurological disorder distinguished by the abnormal synchronous activity of brain neurons. This abnormal activity, consisting of concurrent neuronal electric discharges, causes a nervous attack known as seizure [1]. Epileptic seizures, which are clinically recognized as ictal events, are categorized into two major groups of focal and generalized based on the type of seizure origin [2]. In general, the genesis of a focal seizure is limited to a single hemisphere while a generalized seizure has distributed sources engaging both hemispheres. A focal seizure can be seen in 60 percent of people with epilepsy [2].

Epilepsy is mainly characterized by its seizures or ictal events. However, there are between seizure incidents known as interictal epileptiform discharges (IEDs), which carry significant traits of this brain disorder. Due to the unpredictability of seizures, a thorough investigation of interictal events could enhance our understanding and management of the disease [3].

Due to its simplicity and noninvasive nature, scalp electroencephalography (EEG) recordings remain to this day the first recording modality utilized for diagnosis of epilepsy [3, 4]. Practical considerations, cost-effectiveness, and high temporal resolution make of the EEG recording modality a convenient platform to investigate the epileptogenesis of the disease by studying ictal and interictal episodes in patients with epilepsy [3]. In many studies, interictal EEG intervals were frequently utilized to locate the epileptogenic zone (EZ) in focal epilepsy [5]. In [6], IEDs were used to locate the epileptic source of the high-density scalp EEGs in a population of 38 focal epileptic individuals, and results were precisely correlated with the epileptogenic foci found through seizure onset. However, authors in [7] differentiated the brain areas affected by IEDs and regions that initiated the seizure and concluded the agreement between these zones in 75% of their patients.

Recent studies consider epilepsy as a network disease, which means that in spite of the epileptic focus, there is a network of neuronal activities that contribute to the unusual behavior of the disease [8-10]. It is observed that IEDs as interictal abnormalities make alternations to the default network of the brain [11]. As an example, the effects of spikes in connectivity of mesial temporal lobe epilepsy were tested using frequency domain analysis of EEG signals in [12], which resulted in increased connections in the presence of spikes. A model-based probabilistic connectivity analysis was thus performed during spike-wave discharges in [13], and authors concluded that higher synchrony, larger amplitude, and complex spatial profile were related to the spike activity. In [14], the variation of

epileptic networks during interictal spikes were compared in the right and left temporal lobe epilepsy by applying the electrical source imaging analysis to the high-density EEG recordings. Authors of this study have determined that there was a significant difference in connectivity networks of these two disease types. As another application, directed functional connectivity networks, which were obtained from high-density EEG, were used to differentiate between the three groups of right temporal lobe epilepsy (RTLE), left temporal lobe epilepsy (LTLE) and normal controls [15]. In [16], functional connectivity helped in electrical source imaging to precisely locate the seizure onset area during ictal events. In [17], a directed graph analysis method was adopted to locate the origin of IED activity using intracranial data. Results were corroborated with the clinically determined epileptogenic source. In [18], a network analysis of IEDs over stereotactic EEG data proved a correlation among spike cluster's location and seizure onset zone.

The scalp EEG signal recorded by a single electrode is viewed as a spatiotemporally filtered version of the local field potential (LFP) integrated over an area of about 6 cm^2 or more. Under most conditions, this area will be located near and around the electrode location. Therefore, the relation between electrode signals could lead to the cortical functional relation rather than the structural connections that address biological interactions between neurons. Many connectivity measures have been proposed in the literature to express the dependence among electrodes in the time/frequency domain as well as by utilizing data-driven analyses [19-21]. Phase synchronization based metrics are proved to be more suitable for analyzing the functional connectivity networks since such metrics highlight the synchrony of cortical modules rather than the signal amplitude relations [22, 23]. The synchronization metrics can be realized using linear measurements like coherence, or nonlinear methods that can be adopted, albeit with added computational requirements [24-26]. Some new methods have been developed that suggest the calculation of phase synchrony between two signals using the FFT signal conversion [27, 28]. Since the nonlinear nature of brain signals and the non-stationary features of the EEG can be well explained as complex dynamic oscillators [29], phase synchronization can be well estimated by applying recurrence-based methods to such complex systems [8, 30, 31].

When applying nonlinear methods, data compatibility needs to be examined [32, 33] since a linear correlation or filtered noise in the data might lead to unexpected outcomes [34]. Surrogate data testing is a reliable statistical method that helps evaluate the existence of nonlinearity as well as confirming the significance of the obtained results [29, 32, 35]. This method works based on generating surrogates with similarities to the original data but also with some randomness in its nature [22]. The method tests the desired metric against the null hypothesis of no significant difference among results between original and surrogate data. In fact, the more similar the surrogate is to the original data, the more reliable the results will be [32]. Various techniques are available to generate a surrogate. Surrogate data can be generated easily by shuffling the components of time series (e.g., random shuffling) or applying more advanced methods based on the Fourier transform to maintain some spectral similarities with the original signal [34]. Among all methods that can be used to create a surrogate data, the iterative Amplitude Adjusted Fourier Transform (iAAFT) remains the most widely-used method [34]. The surrogate data testing method has been used in most of the recurrence-based studies, but in this study, we have used this useful statistical test in a novel manner to find suitable parameters that could facilitate the interpretation of results and enhance the analysis.

Source localization using scalp EEG is a technique commonly used to find the epileptogenic area in patients for presurgical evaluation and planning. At this stage, the epileptic focus needs to be localized as accurately as possible. To achieve this goal, high-density EEG and source level directed functional connectivity are proven to be most useful [36, 37]. However, researchers need to deal with the head model selection and inverse solutions that inherently face practical limitations and introduce errors to the 3-D localization process [38-40]. As per our previous study [41], interictal epileptic activity causes high synchronization through the brain with a higher number of strong connections in the connectivity maps. In our previous work, we have investigated the differences between connectivity maps in focal and generalized epilepsy, yielding well-defined regional activities in focal epilepsy and scattered activity in all regions of the brain for the generalized case [42].

Here in this study, we tried to investigate the footprints of the epileptic source in functional connectivity achieved from the standard electrode resolution of the 10-20 EEG system. Since this kind of EEG recording is done at the epilepsy diagnosis stage, we sought to show how functional connectivity can indeed help the neurologist get an idea about the disease type in these early stages of the diagnosis without recourse to a more intensive investigation that may well yield the same outcome. In this research, we have adopted a nonlinear recurrence-based method to estimate the phase synchronization properties of functional brain modules using the interictal EEG time series. We have used a novel technique to find parameters that result in what we termed as significant functional connections. We have investigated the nature of these connectivity maps as a result of focal IEDs in temporal and frontal lobe epileptic patients. These results can be used in concert to the 3D source of seizure onset [43] by simply using interictal EEG activity, and we assert that the interplay between the changes in the connectivity maps in relation to the determined 3D source could eventually aid the validation of the region around and near the 3D source location, which in turn could help gauge the causal effect on these activity maps based on the type of seizure as detailed in Section III.

II. MATERIAL AND METHODS

A. Data

In this study, we have collected the scalp EEG recordings of twenty adult individuals (10 males and 10 females). Nineteen electrodes EEG signals, including Fp1, F7, T3, T5, O1, F3, C3, P3, Fz, Cz, Pz, Fp2, F8, T4, T6, O2, F4, C4 and P4, were recorded based on the 10-20 international placement montage. Signals were digitized using the variable sampling frequencies of 512, 256 and 200 Hz. The signals were all referenced with respect to channel Cz. All participants were diagnosed with

focal epilepsy. The assessment process was performed based on the dipole analysis of selected IEDs, and the specified location(s) were reviewed and confirmed by a group of neurologists at Baptist Hospital of Miami.

The epileptic focus was found in the right/left temporal lobes for ten subjects, for six individuals the epileptic source was diagnosed in the right/left of the frontal area, and the remaining four subjects had bilateral epileptic focus in the temporal or frontal lobes. Table I provides detailed information on the study population. The data was recorded at Baptist Hospital of Miami and subjects were instructed to be relaxed and avoid movement as much as possible during the EEG recording session. The study process was approved by the Institutional Review Board of Florida International University (protocol number: IRB-150247). The EEG data segments considered in this study were those containing interictal discharges as marked by expert neurologists.

B. Preprocessing and Artifact Rejection

Data were preprocessed before segmentation to highlight brain-related activities and minimize the effects of unwanted noise. We applied a 4th order Butterworth band-pass filter with a passing frequency range of 0.5 to 70 Hz. The band-pass filter was applied with zero phase to eliminate the distortion effect of the filter on signals [44]. A notch filter with a frequency of 60Hz is used to suppress the AC line noise. Signal baselines were also removed for all EEG data.

In EEG data analysis, the problem of common sources, whether as volume conduction or active reference electrode affects the connectivity results [24, 45]. A common reference electrode causes a distortion in calculated synchrony among electrodes and results in false phase synchronization values [27]. In our study, we re-referenced the data sets to average montage to overcome this problem. Average reference is normally used in connectivity analysis of EEG to solve this problem [28]. Artifact contaminations such as eye blink, jaw and muscle movements are removed from the data by applying both the principal component analysis (PCA) and independent component analysis (ICA) using EEGLAB software [46].

C. Segmentation

The International Federation of Societies for Electroencephalography and Clinical Neurophysiology (IFSECN) categorizes interictal discharges into four categories of sharp waves, spikes, spike-wave complexes and polyspike-wave complexes [47]. Generally, sharp waves and spikes are associated with focal epilepsy. Since our study population consists mainly of patients with focal epilepsy, we had mostly sharp waves and spikes reflected as the interictal epileptic activity, but there were specific instances where a wave followed the spike.

The filtered, artifact-free EEG data were subdivided into three-second segments as suggested by the neurologist as a means for such segments to be physiologically and computationally meaningful. Epileptiform waves were aligned to the same position in the segment in order to have an equal share of epileptiform activity in the selected segments. One

Table I. Demographic information of participants

Individual ID	Gender	Sampling Rate (Hz)	Epileptic Source Region	Number of Segments
P1	F	512	LT	6
P2	M	512	RT	3
P3	M	512	RT	5
P4	M	512	RT	5
P5	F	512	LT	5
P6	F	512	RT	6
P7	F	512	RT	4
P8	M	512	LT	6
P9	M	512	LT	5
P10	F	512	RT & LFT	5
P11	F	256	LFT & RFT	4
P12	M	512	LF	5
P13	M	512	LFT & RFT	7
P14	M	512	LFT & RFT	10
P15	F	256	RF	5
P16	F	200	LF	5
P17	M	200	LF	3
P18	F	256	RT	5
P19	M	200	RF	4
P20	F	512	LF	6

T: Temporal lobe, F: Frontal lobe, R: Right, L: Left

hundred and four (104) segments of EEG including spike or sharp wave were extracted from the recorded EEG data. These segments were partitioned such that the spike peak is situated in the middle for all extracted segments [41], thus allocating the same amount of time before and after the occurrence of a spike. Fig. 1 illustrates sample data with a spike, a spike followed by a wave and a sharp wave.

D. Functional Connectivity Matrices

The human brain is a complicated system, and EEG signals, as a representation of brain behavior, inherit this complexity. We have applied a nonlinear method, which is based on complex dynamical systems to extract mutual coupling of the individual dynamics of the brain units, and hence it is useful to investigate the behavior of brain dynamics in a reconstructed multi-dimensional space referred to as the phase space.

Recurrence, which is the basic property of complex dynamic systems, is quite beneficial for performing system assessment. It is simply expressed as the return (revisit) of system trajectories to a specific neighborhood or site after a period of time. Recurrence is thus the basis for analyzing phase synchrony between two nonlinear systems. The recurrence plot (RP) can serve as a visualization tool that depicts the behavior of the multidimensional reconstructed trajectory through the advent of recurrence. The RP patterns and features are quantified by a set of techniques, known as recurrence quantification analysis (RQA) [20, 29]. As a further extension of RQA methods, RPs were utilized to estimate the phase synchronization (PS) between the dynamics of two complex systems [48]. This method which is known as the correlation
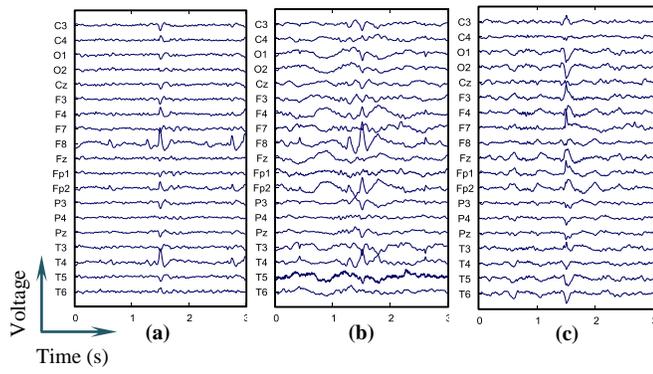
Fig. 1. Sample EEG data segments, (a) Spike with regular background activity from patient P2 where the IED is prominent in F8 and T4. (b) Spike followed by a wave with high background activity from patient P3 where the spike is still noticeable in some channels. (c) Sharp wave with propagation of IED activity in Patient P5 where the spike is not easily localized as in (a).

between probabilities of recurrences (CPR) estimates the PS among signals of the EEG electrodes [30]. In fact, the CPR method finds the synchronized periodic rhythms hidden in the signal and estimates the amount of phase synchrony between them [29]. This characteristic makes this method a strong candidate for analyzing natural complex dynamical oscillators like brain signals.

Based on the dynamical systems theory, the first step is to reconstruct a system trajectory into the phase space. The signal trajectory can be easily rebuilt using time delay theorem as conveyed in [30]. As per this theory, the signal $X = [x_1, x_2, x_3, \ldots, x_N]$ with N entries, reconstructed into a trajectory, y_i, in phase space, can be defined as follows:

$$y_i^T = \begin{bmatrix} x_k\ x_{k+t}\ x_{k+2t}\ \cdots\ x_{k+(m-1)t} \end{bmatrix} \qquad (1)$$

$$m \geq 1, t \geq 1, i = 1, \cdots N \text{ and } k = 1, \cdots, N-(m-1)t$$

Where m defines the embedding dimension, t represents the time delay, and y_i defines the points on the trajectory. The trajectory preserves the topological properties of the original signal; therefore, the spike activities are reflected in these constructed routes [45].

The brain signal trajectories have recursive behavior, meaning the trajectory returns to its neighborhood after a passed time thus establishing a recurrence. The amount and pattern of recurrences explain the signal behavior [45]. Since a direct investigation of trajectory behavior in phase space is not feasible, RPs are developed instead to assess such behavior [43]. Calculation of recurrence is consequently formulated as in (2).

$$R_{i,j} = \Theta\big(\varepsilon - \|\ y_i - y_j\ \|\big) \qquad (2)$$

Based on this relation, the recurrence between points i and j, $R_{i,j}$, is said to occur when the Euclidean distance between these two points in the trajectory is less than a set threshold ε. The function Θ is a Heaviside step function making the resulting value, 0 for no recurrence, or 1 when recurrence occurs. Calculation of recurrence for all points of the trajectory leads to the matrix of recurrence plot.

Various behaviors in trajectories create a variety of specific patterns in the RPs [29]. These specifications, which are extracted by applying the RQA techniques, are used to characterize the different signal states. The periodic rhythms are represented as a long diagonal line in the RPs where the constant vertical distances indicate the period of the signal [29]. In the case of chaotic systems, the diagonal lines are interrupted, and the vertical lines are not consistent, thus representing different periodicities that are concealed in the original signal. If two dynamic systems develop a PS, the vertical distances in both RPs are said to be simultaneous [29]. The RPs diagonal length and the vertical line can be utilized to calculate the probability of recurrence to estimate the PS among electrodes of one EEG segment. This probability of recurrence can be designated as a generalized autocorrelation of the original signal by calculating the number of returns of the trajectory to a specific neighborhood as defined in (3):

$$p(\tau) = \frac{1}{N-\tau}\sum_{i-1}^{N-\tau} R_{i,i+\tau} \qquad (3)$$

Where τ is the time delay and N is the original signal length. The $p(\tau)$ represents the system recurrence (diagonal lines in RPs) based on time delays. If two systems develop phase synchronization, the peaks of $p(\tau)$ of the two signals will coincide. Using this notion, the value of phase synchronization between two-time series can be calculated using the following equation:

$$CPR_{i,j} = \frac{\sum_{\tau=\tau_e}^{\tau_m-1}\big\{(p_i(\tau)-m_i)\cdot(p_j(\tau)-m_j)\big\}}{\sigma_i\sigma_j} \qquad (4)$$

$CPR_{i,j}$ defines the correlation between the probabilities of recurrences, with m_i being the mean and σ_i being the standard deviation of $p_i(\tau)$. The CPR values range from zero when there is no PS between two signals and reaches a value of 1 for the complete PS between the two signals [49]. Calculating all mutual CPR values among all electrodes of one EEG segment establishes the phase synchronization matrix of that EEG segment as in (5).

$$CPR_{N\times N} = \begin{bmatrix} CPR_{1,1} & \cdots & CPR_{1,N} \\ \vdots & \ddots & \vdots \\ CPR_{N,1} & \cdots & CPR_{N,N} \end{bmatrix} \qquad (5)$$

Considering the values of phase synchronization as the strength of connections between brain modules in EEG signals, the brain connectivity matrix is obtained. In fact, two electrodes are considered phase synched, if the CPR value is high (i.e., closer to 1) and are deemed having no coupling if the value of phase synchronization is low (near 0) [48].

E. Parameters Selection and Evaluation

To achieve a reliable connectivity matrix, optimal selection of suitable parameters (time lag, embedding dimension and recurrence threshold) is essential. Various methods have been suggested in the literature to find these appropriate parameters. A very small value for the time lag causes to capture no new information in the successive sampling and creates a redundant situation, while a too large value results in potential information loss [34]. Mutual information, considered sensitive to subtle

changes in the brain, is one of the most popular measures used to determine the optimal time lag [34, 51]. The suitable time lag can be found at the occurrence of the first local minima of the auto-mutual information curve of the signal [34, 51, 52]. On the other hand, the embedding dimension should be large enough to capture the dynamics of the signal but with the caution that very large embedding dimension would make the calculation expensive [48, 51]. The Kth nearest neighbor and Cao's method has been used extensively to find an optimal embedding dimension, [34, 52, 53]. Recurrence threshold is the parameter that affects the advent of recurrence. A value of 10% in space average diameter is assumed empirically appropriate for such a recurrence threshold [29].

Despite the fact that the aforementioned methods are used to find optimal parameters, using these factors is not a guarantee for obtaining what we designate as significant connectivity matrices. To assure the significance of the calculated results, we used a surrogate data testing technique to suggest an algorithm for fine tuning the proper parameters and evaluate the significance of the connectivity matrices. The method works based on generating surrogates of original signals and test for the null hypothesis of similarity between two connectivity matrices generated from original and surrogate signals. Rejection of the null hypothesis is an indication that the connectivity matrix is significant. To generate the surrogate data, we have used the iAAFT method mentioned earlier, which showed more credible results [35]. The number of surrogates calculated for each EEG segment depended on the confidence level we needed for the test. According to the literature [35], for the α level of significance the minimum number of surrogates M, as defined in (6), can be estimated as follows:

$$M = \frac{2K}{\alpha} - 1 \qquad (6)$$

Where K is an integer normally chosen as 1 for simplicity sake. Hence, for a two-sided test with a 95% confidence interval, α will be 0.05, and M will yield 39 surrogates that would be needed in that case.

The connectivity matrices were calculated for the original data as well as for all generated surrogates; then each surrogate connectivity matrix was tested against the original matrix using the Wilcoxon rank sum test. If the rejection rate of the null hypothesis was more than 60%, the original connectivity matrix is considered to be significant.

The surrogate data test was performed for a different combination of parameter values (time lag range of [2~14] and dimension range of [3~10]) to find a set of parameters that lead to significant results. Fig. 2 shows the suggested structure of the algorithm for fine tuning the parameters.

We had chosen the ranges to include the optimal parameters obtained via mutual information and the Cao's method. The final values of the parameters were chosen in a way that connectivity matrices for all of the segments be significant. We
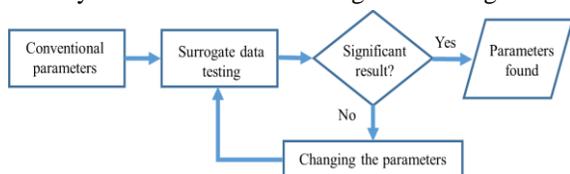
Fig. 2. Structure of the algorithm for fine tuning of the parameters

have started with a time lag of 3 and an embedding dimension of 6, which are assumed computationally optimal; and if the resulting connectivity matrix is not significant, we adjusted these parameters until significant connectivity is obtained. We have reduced the rejection rate of the connectivity matrices to 27.9% by using this method.

III. RESULTS

The connectivity matrices from 104 segments of EEG data have been evaluated for the regional and distant patterns related to the interictal epileptiform discharges (IED). Parameters were adjusted to yield significant functional connectivity values using the surrogate data method, and the significance of the connection values was assessed. There were 4 EEG segments which were excluded from our study as they did not yield significant connectivity matrices for the assumed range of parameters. The remaining 100 connectivity matrices were thus considered for the assessment of the epileptogenic zone activity using functional connectivity maps.

To highlight the behavior of a given epileptogenic zone in the connectivity maps, we counted the activity of each region as local connectivity and the strong links that connected two local areas as distant connections. We have divided the brain cortex into the six functional areas as depicted in Fig. 3. Table II lists the placement of the electrodes within these brain areas.

We investigated the relationship between local areas to obtain the propagation patterns resulting from the IED activity. We considered couplings between the left frontal and left temporal (FL-TL), right frontal and right temporal (FR-TR), left temporal and left parietal (TL-PL), right temporal and right parietal (TR-PR), as the ipsilateral inter-relation of local zones, and the inter-hemispheric relationships are also checked by observing links between the left and right frontal regions (FL-FR), and left and right temporal regions (TL-TR).

A. Threshold selection and assessment of connectivity maps

We separated the links associated with the IED activity by thresholding the connectivity matrices and generating the connectivity maps. The PS value among electrodes ranged from 0 (indicating no synchronization) to 1 (complete coupling). Based on the literature, the CPR value of 0.5 or 0.6 denotes the start of synchrony among the two systems [30, 50]. Therefore, a higher threshold is deemed sufficient to best-represent a well-established link. In our application, the segment's background activity should be considered since there was some variability among segments belonging to the same patient. Since the IED activity is associated with stronger links [42], adjustments of the threshold needed to be made in a way to delineate the IED-related connections. Therefore, we considered a general threshold of 0.75 as the minimum value for such connections. It means that two electrodes were considered connected if the value of CPR was higher than or equal to 0.75 and all lower values are assumed as no connection between aforesaid electrodes. Given that thresholds are subjective, we assumed normal distributions of the connection strengths in the connectivity patterns and made use of the mean (μ), standard deviation (σ) and upper percentile (z) measures to determine an adjusted threshold based on the following formula:
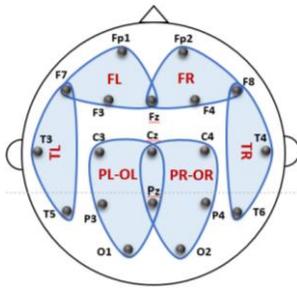
Fig 3. The different local brain regions considered and related placement of electrodes

Table II. Six brain local regions and related electrodes

Region name	Abbreviation	Electrodes
Left Frontal	FL	Fp1, Fz, F3, F7
Right Frontal	FR	Fp2, Fz, F4, F8
Left Temporal	TL	F7, T3, T5
Right Temporal	TR	F8, T4, T6
Left Parietal and Left Occipital	PL-OL	C3, Cz, P3, Pz, O1
Right Parietal and Right Occipital	PR-OR	C4, Cz, P4, Pz, O2

$$T_a = \mu + z\sigma \qquad (7)$$

$$\begin{cases} if\ T_a \leq 0.75, then\ T = 0.75 \\ if\ T_a > 0.75, then\ T = T_a \end{cases}$$

Where T_a is the adjusted value and T is the threshold. To visualize better this problem, Fig. 4 compares two segments from a same individual (P6) with different background activity. As depicted in part (a), the same threshold of 0.75 is applied to the connectivity matrices and shows a full connectivity map for segment 2. In part (b) the connection distribution for the two segments were shown in the same plot, it can be observed that segment 2 resulted in higher value connections. In Part (c) the connectivity maps are instead shown with the adjusted threshold formula in (7), where it can be seen that the two connectivity maps are more homogeneous with regards to connection density.

To correlate the region's activity with the epileptogenic zone, we quantified the activity of local regions by calculating the activity percentage for each local area. Activity percentage is obtained by dividing the number of available connections over the number of possible connections for that area as formulated in (8):

$$PA_x = \frac{l_x}{L_t} \times 100 \qquad (8)$$

Where PA_x denotes the percentage activity for region x. The value of l_x defines the number of available connections in the region and L_t is the number of possible connections in the relevant local region. Local brain areas were ranked based on the percentage activity to determine the most active regions.

In our study population, the IED with the highest voltage field was observed in electrodes that are located in the epileptogenic zone or nearby areas. However, there were three cases related to patients P5, P7, and P9 where electrodes with the largest epileptic activity were not as prominent with respect to other electrodes. Referring back to Fig 1, the different EEG

segments clearly show the complexity of such signals and the different ways interictal spikes manifest themselves. For example, Fig 1(a) shows a sample data segment of patient P2 with clear spike activity observed in F8 and T4 and with a relatively smooth EEG background activity, but in Fig. 1 (b), showing a segment from patient P3, while one of the spikes is prominent, most others seem overwhelmed by the higher EEG background activity. Spikes showed in Fig. 1 (c) of patient P5 seem to be more uniform across the channels, but the spikes are just slightly more prominent than the EEG background activity. These different ways that spikes manifest themselves underlines the importance of having a mathematically derived threshold as expressed in (7) that could provide uniformity in the way to express the connectivity maps and to allow for more meaningful comparisons and assessments.

We have thus compared the local brain activity statistically by combining the regional synchronization values of several segments. The non-parametric statistical test of Kruskal Wallis (analysis of variance with the null hypothesis of the same median) has been conducted per individual. These tests were followed by the post-hoc analysis with Bonferroni correction for the significance value, to highlight the areas which were significantly different. Table III lists the test results with the calculated P-values.

B. Individuals with temporal lobe epileptic focus

We have investigated the individuals grouped based on the same location of the epileptic source. In patients with the epileptogenic zone in the left temporal area (P1, P5, P8, and P9), TL was highlighted as an expected active zone. In addition, we observed that the frontal areas (Left and Right) also exhibit high connections. In fact, in all patients, except for P8, the frontal lobes show slightly higher activity than the left temporal lobe. The right temporal zone was the next active zone. Strong distant links between left and right frontal lobes (FL-FR) were observed in all individuals and strong left temporal-frontal links (FL-TL) were also observed in P1, P5, and P8.

In cases with a focus in the right temporal (P2, P3, P4, P6, P7, and P18), TR was indeed the region found to have the highest activity. In addition, TL and FR were also very active lobes. The FL region did not show high activity in all patients, but only in P4, P6 and P7. The PL region was found to be an active region in all cases except for P7 and P18. Strong connections were observed in both TL and TR lobes. Unlike the left temporal group, we did not observe solid connections between the frontal areas, while the FR and TR regions were still strongly linked as was expected given the observation already made for the left temporal focus. Statistically, we did not observe significant differences among the activity between TR, FR and TR, TL.

C. Individuals with Frontal lobe epileptic focus

In the group with left frontal focus (P12, P16, P17, and P20), high activity was observed in both FL and TL in all patients except for P12. There was also a propagation of the activity to FR and TR. Strong distant links were also observed between FL and TL. The two hemispheres were connected through temporal

lobes (P12 and P16) or frontal lobes (P17 and P20). Statistically, no significant difference was observed between FL, TL, FR and TR zones, while parietal regions were significantly different.

In patients with a focus on the right frontal (P15 and P19), the FR, FL, and TL regions were found to be highly active with TR being the next active zone. The epileptic source assessment of these two patients showed activity in the left hemisphere which conforms to the high synchrony achieved in connectivity maps. Strong distant links connected frontal areas in both hemispheres and frontal-temporal regions in the left hemisphere. Unlike the left frontal focus group, we did not observe strong connections between FR and TR. No significant difference in synchronization activity of FR, TR, FL, and TL was observed, while activity in FL, TL and FR was significantly different from those in PL-OL and PR-OR.

D. Patients with bilateral focus

For Patients with bilateral focus (P10, P11, P13, and P14), we considered segments with the same active focus to find the source-relevant patterns. For patients P10, P11 and P14, the activity of one source were dominant in the EEG segment, while for patient P13 both epileptic foci were active in all segments; therefore, we considered all segments in the same group.

In cases that the right focus was active, we observed high activity in FR, TR, FL, and TL in all patients, while in P10, PL-OL was highly active. In all these cases, strong connections linked the contralateral temporal and frontal regions (TL-TR and FL-FR)

When a left source was active FL, TL and FR were the most active regions. The activity extends to TR lobe in case of P14 and P10. Here, the interhemispheric stronger link was FL-FR rather than TL-TR. Statistically, significant activity was observed among parietal and frontal areas and not among frontal and temporal areas.

To visualize these connections in relation to their spatial locations on the scalp, we plotted the connectivity matrices on the head map after pruning them with the threshold. The strength of connections was depicted by color codes representing dark red, as a very strong connection and dark blue as weak coupling. Fig. 5 shows the activities in six local areas with relevant distant regional connections for cases with right temporal, left frontal and a bilateral patient. The comparison of the local and distant activities in terms of the average activity percentage across individuals with the same epileptic focus is also shown in Fig. 6, and these results are summarized in our discussion section in parts B, C and D.

In our population study, we have recognized three patterns based on the location of the epileptic focus. In General, the epileptogenic focus located in the temporal or frontal lobes irritates both ipsilateral and contralateral frontal and temporal areas, but the pattern varies depending on the location of the focus. The left temporal focus tends to expand to contralateral hemisphere through the frontal zones, while evidence indicates right temporal sources engage the other hemisphere through temporal links. Likewise, the frontal source pattern affects both,

Statistical metric	Segment 1	Segment 2
Mean	0.67	0.8
Standard deviation	0.104	0.075
Upper percentile	0.73	0.86

(b)
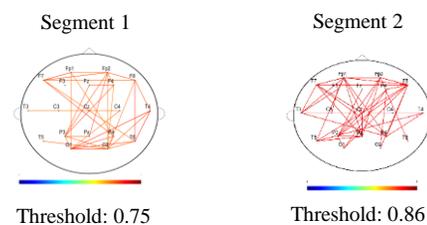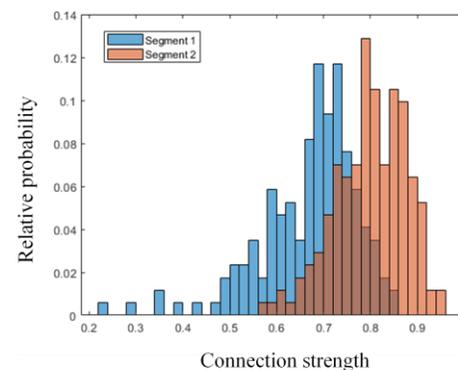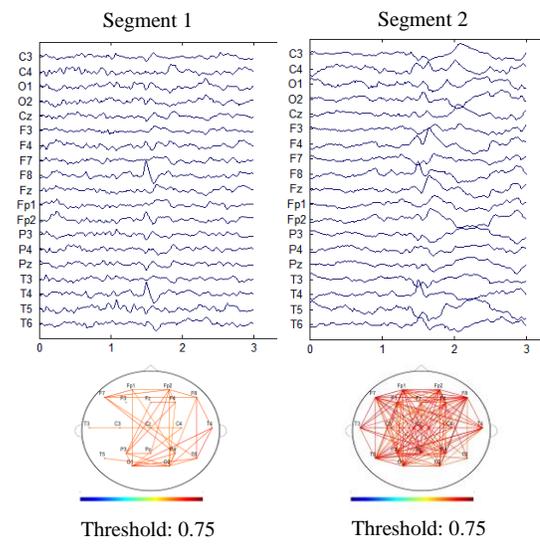
Fig. 4. The comparison of the effect of the adjusting the threshold on the connectivity maps. (a) Shows two segments of patient P6 with different background (spike peak to signal mean difference for segment 1 is 0.0933 and for segment 2 is 0.0751) and relevant connectivity maps with general threshold of 0.75. (b) represents the connection distribution and statistics for the two connectivity matrices. (c) Shows the two connectivity maps with the adjusted threshold for segment 2.

left and right frontal and temporal zones, but the link can be either through TL-TR or FL-FR. In frontal patterns, we have seen more significant differences in synchronization among frontal-temporal regions and parietal areas. This can happen since frontal sources are less likely to affect the parietal zones,

Table III. Regional activity statistical test results

ID	Epileptic Source	P-value	ID	Epileptic Source	P-value
P1	LT	3.68e-07	P11(Right)	R FT	7.73e-02*
P2	RT	1.05e-04	P12	LF	6.41e-01*
P3	RT	2.46e-08	P13	L/R FT	1.17e-02
P4	RT	1.30e-03	P14(Left)	L FT	3.79e-03
P5	LT	2.80e-02*	P14(Right)	R FT	5.79e-03
P6	RT	1.10e-03	P15	RF	1.55e-07
P7	RT	5.40e-03	P16	LF	8.58e-06
P8	LT	1.04e-01*	P17	LF	1.80e-03
P9	LT	3.84e-02*	P18	RT	6.13e-08
P10	RT & LFT	1.80e-01*	P19	RF	8.06e-15
P11(Left)	L FT	1.84e-06	P20	LF	7.28e-05

* Not significant

while this might not be the case in temporal sources. Based on our study, bilateral patterns depend on the single or simultaneous activation of the two sources.

We have extracted the propagation patterns of frontal and temporal focal epilepsies utilizing the interictal EEG recordings. The interictal data is the strength of our study since interictal recordings are easier to get in EEG than actual seizure events. On the other hand, separating good spikes with minimum background activity is a limiting factor. Although this study is helpful in the diagnosis of the disease, the method is only based on analysis of the interictal data in the early diagnosis stages. This is why we need future investigations to make it more engaging for enhancing clinical decisions. As our research group continues to see patients in another IRB approved study to perform EEG-triggered fMRI, where EEG recordings are done simultaneously as a patient is inside an MRI machine, it will be extremely important to validate such work by looking at the BOLD effect as well as the default mode network in resting-state fMRI to gauge such connectivity links and any potential disruptions due to the position of the 3D source and the interictal spikes that have triggered the fMRI process.

IV. CONCLUSION

A nonlinear data-driven method is applied to scalp EEG signals to estimate the phase coupling among brain cortical nodes. Functional connectivity maps were explored both locally and in terms of how the epileptogenic zone can affect distant areas of the brain. Local links were investigated concerning six brain regions (left and right frontal, left and right temporal, left and right parietal and occipital).

Relationships between the local areas were investigated through distant connections. Moreover, obtaining the activity percentages allowed us to assess the regional activities and the most active areas for every connectivity map.

The comparison between activities of local areas indicates that the region associated with the epileptic foci results in high coupling in their corresponding connectivity maps. In addition to the affected temporal or frontal area, we have observed high synchrony in the frontal zone of the affected hemisphere.

Furthermore, we observed strong links connecting the active distant regions resulting in stimulation of temporal and frontal areas of the opposite hemisphere. Interestingly, we have found different propagation patterns based on the hemisphere that contains the epileptic source. In general, we have observed that epileptic activity in temporal and frontal area irritates both hemispheres in both the temporal and frontal zones. These findings enhance our perception of the epileptic brain mechanism as a network disease, which through the different activity patterns could help assess brain areas that are most affected.

Overall, our contributions can be summarized as follows:
- Interictal data is used to determine brain activity patterns and the effects it has on distant areas.
- A nonlinear data-driven method is used to estimate phase synchrony using a time domain analysis.
- A method is proposed for finding parameters to ensure that significant connectivity matrices are obtained.
- A new thresholding method is proposed based on the distribution of the connection values in order to overcome the intra-variability in the EEG segments and provide for more meaningful comparisons between brain connectivity maps.

REFERENCES

[1] R. S. Fisher, W. v. E. Boas, W. Blume, C. Elger, P. Genton, P. Lee and J. Engel, "Epileptic seizures and epilepsy: definitions proposed by the International League Against Epilepsy (ILAE) and the International Bureau for Epilepsy (IBE)," *Epilepsia,* vol. 46, *(4),* pp. 470-472, 2005.

[2] National Institute of Neurological Disorders and Stroke (US). Office of Communications and Public Liaison, *The Epilepsies and Seizures: Hope through Research.* Department of Health & Human Services, NIH, National Institute of Neurological Disorders and Stroke, 2015.

[3] S. J. Smith, "EEG in the diagnosis, classification, and management of patients with epilepsy," *J. Neurol. Neurosurg. Psychiatry.,* vol. 76 Suppl 2, pp. 7, Jun, 2005.

[4] U. R. Acharya, S. V. Sree, G. Swapna, R. J. Martis and J. S. Suri, "Automated EEG analysis of epilepsy: a review," *Knowledge-Based Syst.,* vol. 45, pp. 147-165, 2013.

[5] P. Mégevand and M. Seeck, "Electroencephalography, magnetoencephalography and source localization: their value in epilepsy," *Current Opinion in Neurology,* vol. 31, *(2),* pp. 176, 2018.

[6] P. Mégevand, L. Spinelli, M. Genetti, V. Brodbeck, S. Momjian, K. Schaller, C. M. Michel, S. Vulliemoz and M. Seeck, "Electric source imaging of interictal activity accurately localises the seizure onset zone," *Journal of Neurology, Neurosurgery, and Psychiatry,* vol. 85, *(1),* pp. 38-43, 2014.

[7] F. Bartolomei, A. Trébuchon, F. Bonini, I. Lambert, M. Gavaret, M. Woodman, B. Giusiano, F. Wendling and C. Bénar, "What is the concordance between the seizure onset zone and the irritative zone? A SEEG quantified study," *Clinical Neurophysiology,* vol. 127, *(2),* pp. 1157-1162, 2016..

[8] K. Lehnertz, S. Bialonski, M. Horstmann, D. Krug, A. Rothkegel, M. Staniek and T. Wagner, "Synchronization phenomena in human epileptic brain networks," *J. Neurosci. Methods,* vol. 183, *(1),* pp. 42-48, 2009.

[9] C. Wilke, G. Worrell and B. He, "Graph analysis of epileptogenic networks in human partial epilepsy," *Epilepsia,* vol. 52, *(1),* pp. 84-93, 2011.

[10] Peng Xu, Xiuchun Xiong, Qing Xue, Peiyang Li, Rui Zhang, Zhenyu Wang, P. A. Valdes-Sosa, Yuping Wang and Dezhong Yao, "Differentiating Between Psychogenic Nonepileptic Seizures and Epilepsy Based on Common Spatial Pattern of Weighted EEG Resting Networks," *Tbme,* vol. 61, *(6),* pp. 1747-1755, 2014.

This article has been accepted for publication in a future issue of this journal, but has not been fully edited. Content may change prior to final publication. Citation information: DOI 10.1109/TBME.2019.2919263, IEEE Transactions on Biomedical Engineering

TBME-01355-2018   9

(a)

(b)
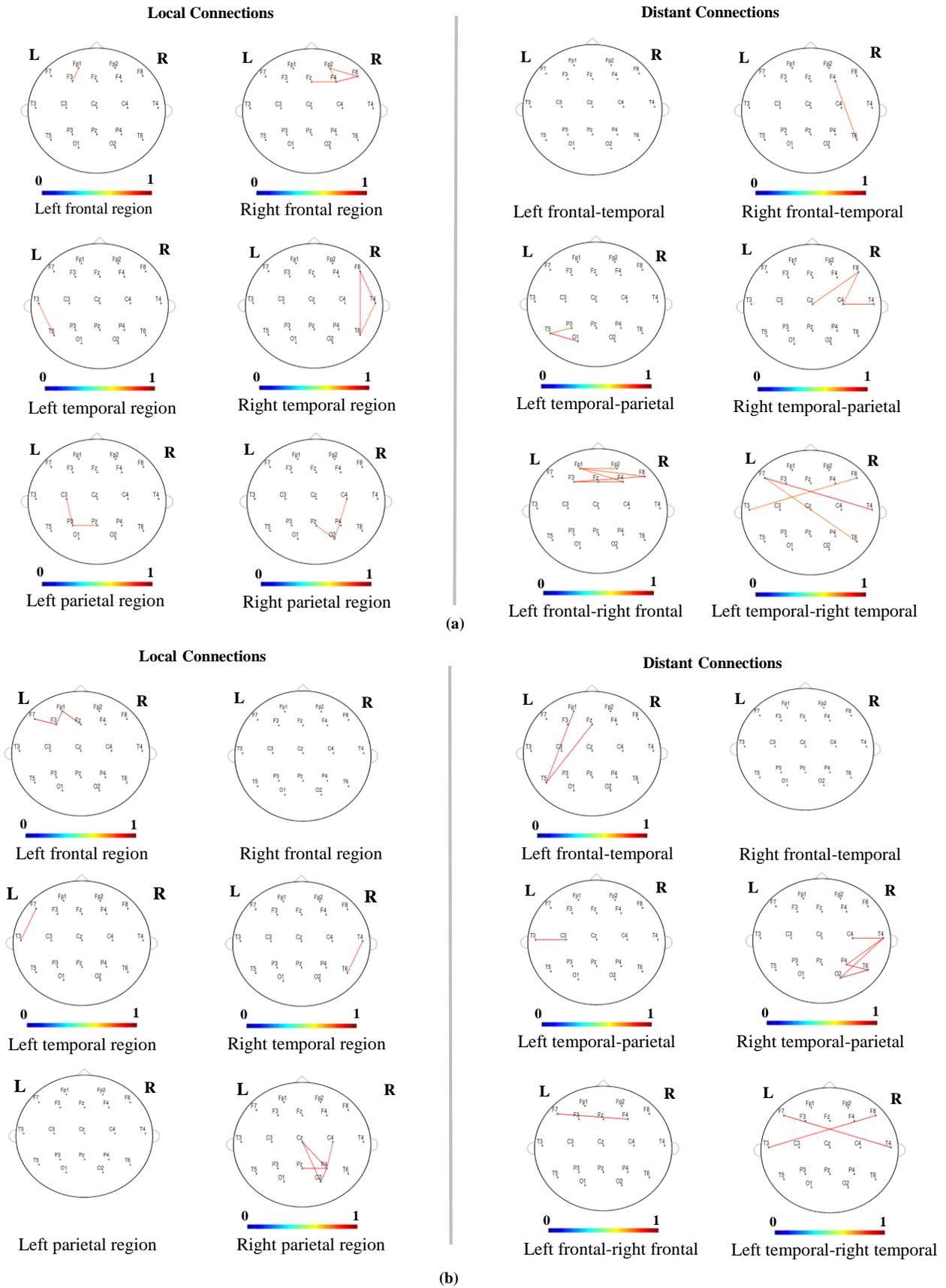
Fig5. Head map connectivity plot of local and distant regions resulting from a sample EEG segment of (a) P4 with right temporal epileptic focus, (b) P12 with epileptic focus in left frontal and (c) P10 with bilateral focus (RT-LFT) and right focus is active for this segment. Note: only strong connections are shown.
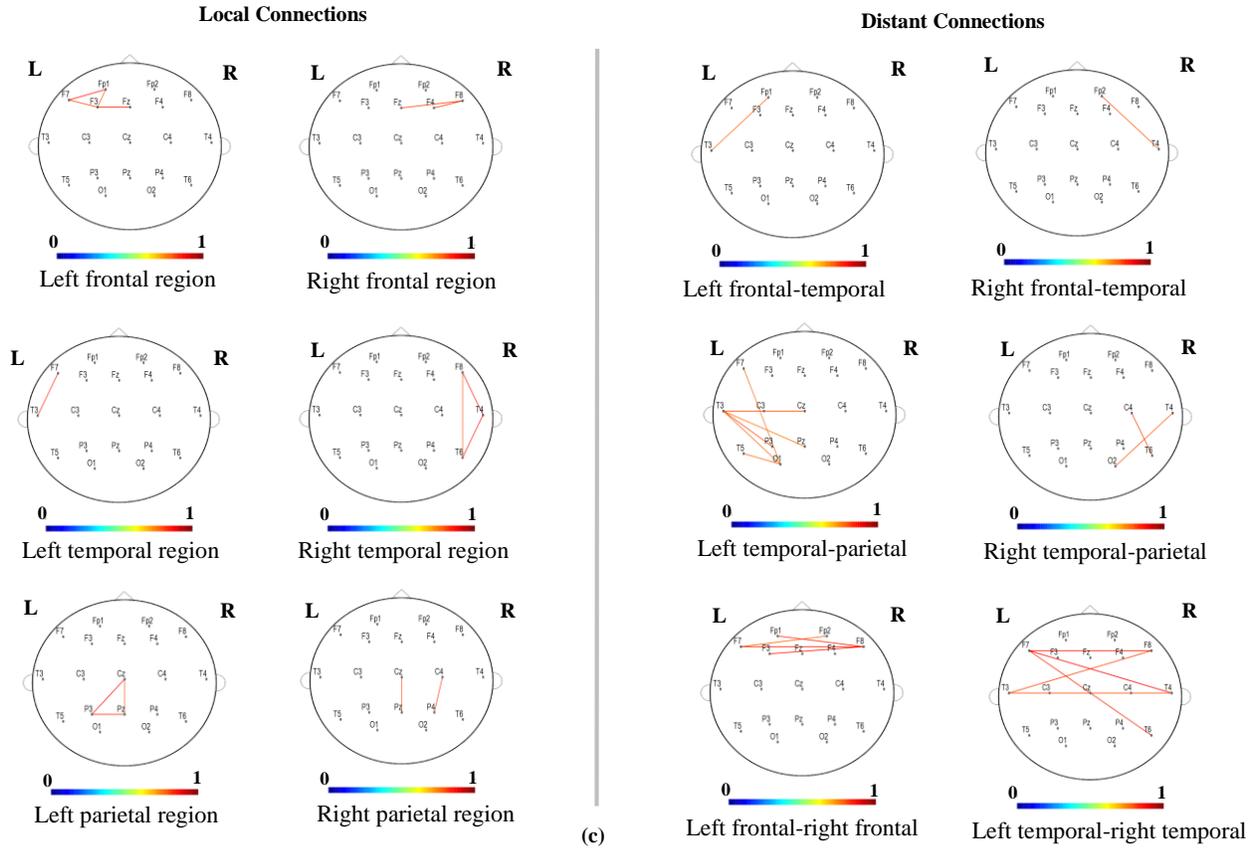
Fig. 5 (Cont.) Head map connectivity plot of local and distant regions resulting from a sample EEG segment of (a) P4 with right temporal epileptic focus, (b) P12 with epileptic focus in left frontal and (c) P10 with bilateral focus (RT-LFT) and right focus is active for this segment. Note: only strong connections are shown.
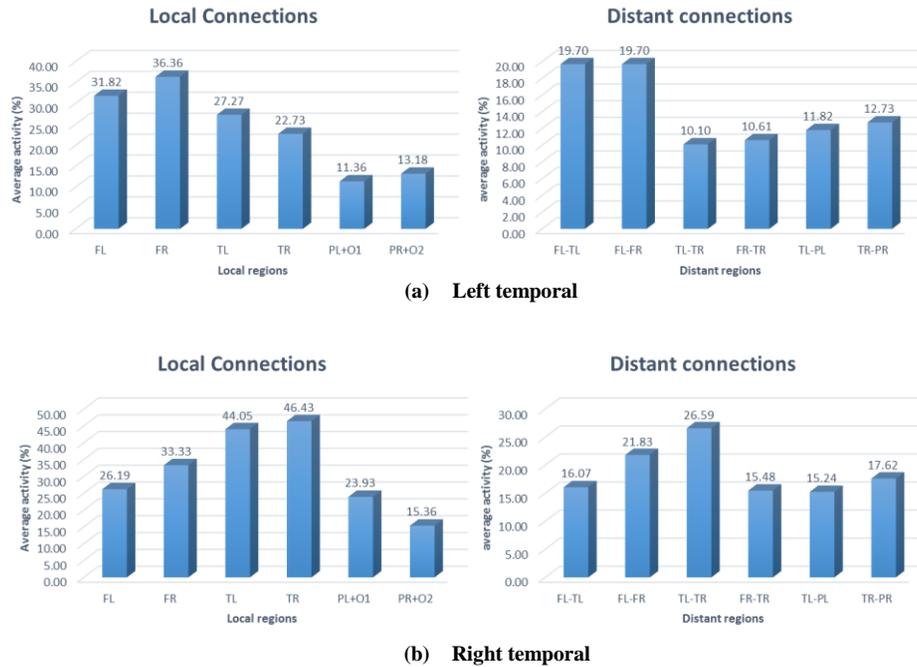
Fig. 6. The bar plot of the average activity percentage across patients grouped with the same epileptic focus. Segments with same active epileptic source are grouped together.

This article has been accepted for publication in a future issue of this journal, but has not been fully edited. Content may change prior to final publication. Citation information: DOI 10.1109/TBME.2019.2919263, IEEE Transactions on Biomedical Engineering

TBME-01355-2018   11

(c) Left frontal

(d) Right frontal

(e) Bilateral focus (left source is active)

(f) Bilateral focus (right source is active)

(g) Bilateral focus (Both sources are active)
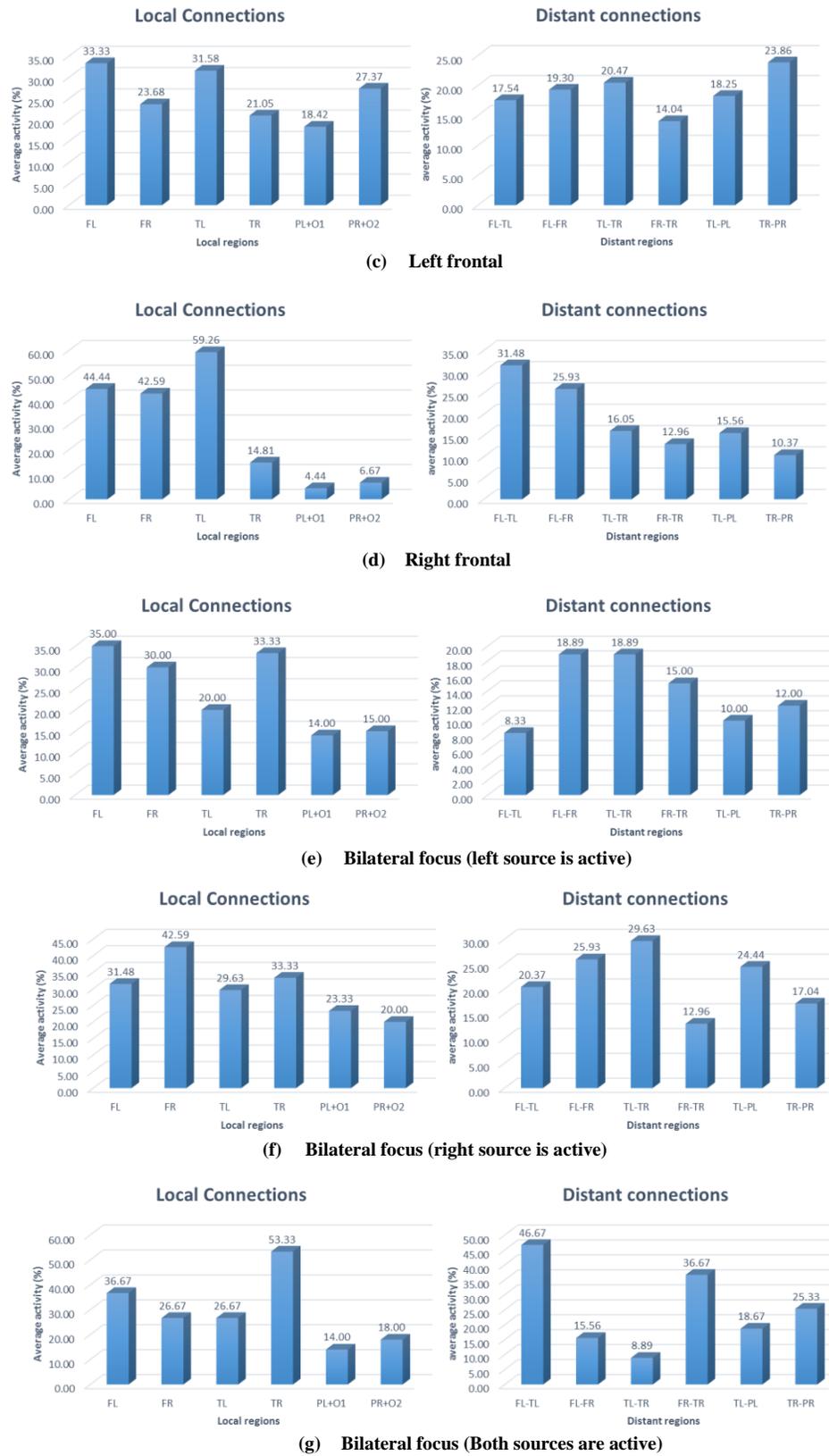
Fig. 6. (Cont.) The bar plot of the average activity percentage on patients with temporal and frontal epileptic focus. Segments with same active epileptic source are grouped together.

[11] E. van Diessen, W. M. Otte, C. J. Stam, K. P. Braun and F. E. Jansen, "Electroencephalography based functional networks in newly diagnosed childhood epilepsies," *Clinical Neurophysiology,* vol. 127, *(6),* pp. 2325-2332, 2016.

[12] G. Bettus, F. Wendling, M. Guye, L. Valton, J. Régis, P. Chauvel and F. Bartolomei, "Enhanced EEG functional connectivity in mesial temporal lobe epilepsy," *Epilepsy Res.,* vol. 81, *(1),* pp. 58-68, 2008.

[13] P. N. Taylor, M. Goodfellow, Y. Wang and G. Baier, "Towards a large-scale model of patient-specific epileptic spike-wave discharges," *Biol. Cybern.,* vol. 107, *(1),* pp. 83-94, 2013.

[14] A. Coito, G. Plomp, M. Genetti, E. Abela, R. Wiest, M. Seeck, C. M. Michel and S. Vulliemoz, "Dynamic directed interictal connectivity in left and right temporal lobe epilepsy," *Epilepsia,* vol. 56, *(2),* pp. 207-217, 2015.

[15] T. Verhoeven, A. Coito, P. van Mierlo, M. Seeck, C. Michel, G. Plomp, J. Dambre and S. Vulliemoz, "Using random forest for diagnosis and lateralization of temporal lobe epilepsy from EEG-based directed functional connectivity," in *12th European Congress on Epileptology,* 2016, pp. 64.

[16] W. Staljanssens, G. Strobbe, R. Van Holen, V. Keereman, S. Gadeyne, E. Carrette, A. Meurs, F. Pittau, S. Momjian, M. Seeck, P. Boon, S. Vandenberghe, S. Vulliemoz, K. Vonck and P. van Mierlo, "EEG source connectivity to localize the seizure onset zone in patients with drug resistant epilepsy," *NeuroImage: Clinical,* vol. 16, pp. 689-698, 2017..

[17] L. Amini, C. Jutten, S. Achard, O. David, H. Soltanian-Zadeh, G. A. Hossein-Zadeh, P. Kahane, L. Minotti and L. Vercueil, "Directed Differential Connectivity Graph of Interictal Epileptiform Discharges," *Tbme,* vol. 58, *(4),* pp. 884-893, 2011.

[18] S. Meesters, P. Ossenblok, A. Colon, L. Wagner, O. Schijns, P. Boon, L. Florack and A. Fuster, "Modeling of intracerebral interictal epileptic discharges: Evidence for network interactions," *Clinical Neurophysiology,* vol. 129, *(6),* pp. 1276-1290, 2018..

[19] B. Horwitz, "The elusive concept of brain connectivity," *Neuroimage,* vol. 19, *(2),* pp. 466-470, 2003.

[20] V. Sakkalis, "Review of advanced techniques for the estimation of brain connectivity measured with EEG/MEG," *Comput. Biol. Med.,* vol. 41, *(12),* pp. 1110-1117, 2011.

[21] K. Ansari-Asl, J. -. Bellanger, F. Bartolomei, F. Wendling and L. Senhadji, "Time-frequency characterization of interdependencies in nonstationary signals: application to epileptic EEG," *Tbme,* vol. 52, *(7),* pp. 1218-1226, 2005.

[22] Junfeng Sun, Xiangfei Hong and Shanbao Tong, "Phase Synchronization Analysis of EEG Signals: An Evaluation Based on Surrogate Tests," *Tbme,* vol. 59, *(8),* pp. 2254-2263, 2012.

[23] T. Sobayo, A. S. Fine, E. Gunnar, C. Kazlauskas, D. Nicholls and D. J. Mogul, "Synchrony Dynamics Across Brain Structures in Limbic Epilepsy Vary Between Initiation and Termination Phases of Seizures," *Tbme,* vol. 60, *(3),* pp. 821-829, 2013.

[24] C. J. Stam, G. Nolte and A. Daffertshofer, "Phase lag index: Assessment of functional connectivity from multi channel EEG and MEG with diminished bias from common sources," *Hum. Brain Mapp.,* vol. 28, *(11),* pp. 1178-1193, 2007.

[25] S. N. Kalitzin, J. Parra, D. N. Velis and F. H. L. da Silva, "Quantification of Unidirectional Nonlinear Associations Between Multidimensional Signals," *Tbme,* vol. 54, *(3),* pp. 454-461, 2007..

[26] Yifan Zhao, S. A. Billings, Hua-Liang Wei and P. G. Sarrigiannis, "A Parametric Method to Measure Time-Varying Linear and Nonlinear Causality With Applications to EEG Data," *Tbme,* vol. 60, *(11),* pp. 3141-3148, 2013.

[27] K. Majumdar, "An FFT based measure of phase synchronization," *arXiv Preprint Q-Bio/0612004,* 2006.

[28] H. M. Golshan, A. O. Hebb, S. J. Hanrahan, J. Nedrud and M. H. Mahoor, "An FFT-based Synchronization Approach to Recognize Human Behaviors using STN-LFP Signal," *arXiv Preprint arXiv:1612.08780,* 2016.

[29] N. Marwan, M. C. Romano, M. Thiel and J. Kurths, "Recurrence plots for the analysis of complex systems," *Physics Reports,* vol. 438, *(5),* pp. 237-329, 2007.

[30] M. Lakshmanan and D. V. Senthilkumar, "Transition from phase to generalized synchronization," in *Dynamics of Nonlinear Time-Delay Systems*Anonymous Springer, Berlin, Heidelberg, 2011, pp. 201-226

[31] D. Rangaprakash, X. Hu and G. Deshpande, "Phase synchronization in brain networks derived from correlation between probabilities of recurrences in functional MRI data," *Int. J. Neural Syst.,* vol. 23, *(02),* pp. 1350003, 2013.

[32] K. Natarajan, R. Acharya, F. Alias, T. Tiboleng and S. K. Puthusserypady, "Nonlinear analysis of EEG signals at different mental states," *BioMedical Engineering OnLine,* vol. 3, *(1),* pp. 7, 2004.

[33] T. Schreiber and A. Schmitz, "Surrogate time series," *Physica D,* vol. 142, *(3–4),* pp. 346-382, 2000.

[34] N. Puthanmadam Subramaniyam, "Recurrence network analysis of EEG signals," 2016.

[35] T. Gautama, D. P. Mandic and M. M. Van Hulle, "Indications of nonlinear structures in brain electrical activity," *Physical Review E,* vol. 67, *(4),* pp. 046204, 2003.

[36] A. Sohrabpour, Shuai Ye, G. A. Worrell, Wenbo Zhang and Bin He, "Noninvasive Electromagnetic Source Imaging and Granger Causality Analysis: An Electrophysiological Connectome (eConnectome) Approach," *Tbme,* vol. 63, *(12),* pp. 2474-2487, 2016.

[37] A. Coito, C. M. Michel, P. van Mierlo, S. Vulliemoz and G. Plomp, "Directed Functional Brain Connectivity Based on EEG Source Imaging: Methodology and Application to Temporal Lobe Epilepsy," *Tbme,* vol. 63, *(12),* pp. 2619-2628, 2016.

[38] S. A. H. Hosseini, A. Sohrabpour and B. He, "Electromagnetic source imaging using simultaneous scalp EEG and intracranial EEG: An emerging tool for interacting with pathological brain networks," *Clinical Neurophysiology,* vol. 129, *(1),* pp. 168-187, 2018.

[39] C. Wilke, Lei Ding and Bin He, "Estimation of Time-Varying Connectivity Patterns Through the Use of an Adaptive Directed Transfer Function," *Tbme,* vol. 55, *(11),* pp. 2557-2564, 2008.

[40] B. L. P. Cheung, R. Nowak, Hyong Chol Lee, W. Drongelen and B. D. Veen, "Cross Validation for Selection of Cortical Interaction Models From Scalp EEG or MEG," *Tbme,* vol. 59, *(2),* pp. 504-514, 2012.

[41] H. Rajaei, M. Cabrerizo, P. Janwattanapong, A. Pinzon-Ardila, S. Gonzalez-Arias and M. Adjouadi, "Connectivity maps of different types of epileptogenic patterns," in *Proceedings of 38Th Annual International Conference of the IEEE Engineering in Medicine and Biology Society 2016 (IEEE EMBC'16),* Orlando,FL, 2016, pp. 1019,1020,1021.

[42] H. Rajaei, M. Cabrerizo, P. Janwattanapong, A. Pinzon, S. Gonzalez-Arias, A. Barreto and M. Adjouadi, "Connectivity dynamics of interictal epileptiform activity," in *Bioinformatics and Bioengineering (BIBE), 2017 IEEE 17th International Conference,* 2017, pp. 425-430.

[43] C. Mercedes, M. Adjouadi, M. Ayala and M. Tito, "Pattern extraction in interictal EEG recordings towards detection of electrodes leading to seizures." *Biomed. Sci. Instrum.,* vol. 42, pp. 243-248, 2005.

[44] H. Rajaei, M. Cabrerizo, S. Sargolzaei, A. Pinzon-Ardila, S. Gonzalez-Arias and M. Adjouadi, "Pediatric epilepsy: Clustering by functional connectivity using phase synchronization," in *Biomedical Circuits and Systems Conference (BioCAS), 2015 IEEE,* 2015, pp. 1-4.

[45] R. Guevara, J. L. P. Velazquez, V. Nenadovic, R. Wennberg, G. Senjanović and L. G. Dominguez, "Phase synchronization measurements using electroencephalographic recordings," *Neuroinformatics,* vol. 3, *(4),* pp. 301-313, 2005.

[46] A. Delorme and S. Makeig, "EEGLAB: an open source toolbox for analysis of single-trial EEG dynamics including independent component analysis," *J. Neurosci. Methods,* vol. 134, *(1),* pp. 9-21, 2004.

[47] S. Noachtar, C. Binnie, J. Ebersole, F. Mauguière, A. Sakamoto and B. Westmoreland, "A glossary of terms most commonly used by clinical electroencephalographers and proposal for the report form for the EEG findings. The International Federation of Clinical Neurophysiology." *Electroencephalogr Clin Neurophysiol Suppl,* vol. 52, pp. 21-41, 1999.

[48] D. Rangaprakash, "Connectivity analysis of multichannel EEG signals using recurrence based phase synchronization technique," *Comput. Biol. Med.,* vol. 46, pp. 11-21, 2014.

[49] D. Rangaprakash and N. Pradhan, "Study of phase synchronization in multichannel seizure EEG using nonlinear recurrence measure," *Biomedical Signal Processing and Control,* vol. 11, pp. 114-122, 2014.

[50] B. Schelter, M. Winterhalder and J. Timmer, *Handbook of Time Series Analysis: Recent Theoretical Developments and Applications.* John Wiley & Sons, 2006.

[51] J. P. Zbilut and C. L. Webber, "Recurrence quantification analysis," *Wiley Encyclopedia of Biomedical Engineering,* 2006.

[52] B. J. West, "Fractal Physiology and Chaos in Medicine (Studies of Nonlinear Phenomena in Life Science, Vol 1)," 1991.

[53] L. Cao, "Practical method for determining the minimum embedding dimension of a scalar time series," *Physica D: Nonlinear Phenomena,* vol. 110, *(1),* pp. 43-50, 1997.